THE UNIVERSITY OF MICHIGAN

COLLEGE OF ENGINEERING
Department of Applied Mechanics & Engineering Science

Technical Report No. 14

TESTING TECHNIQUES FOR DETERMINING STATIC MECHANICAL PROPERTIES OF PNEUMATIC TIRES

R. N. Dodge
R. B. Larson
S. K. Clark
G. H. Nybakken

supported by:

NATIONAL AERONAUTICS AND SPACE ADMINISTRATION
GRANT No. NGL 23-005-010
WASHINGTON, D.C.

administered through:

DIVISION OF RESEARCH DEVELOPMENT AND ADMINISTRATION ANN ARBOR

July 1973

TABLE OF CONTENTS

LIST OF ILLUSTRATIONS

LIST OF ILLUSTRATIONS (Concluded)

TESTING TECHNIQUES FOR DETERMINING STATIC MECHANICAL PROPERTIES OF PNEUMATIC TIRES

By R. N. Dodge, R. B. Larson, S. K. Clark, and G. H. Nybakken

SUMMARY

Fore-aft, lateral, and vertical spring rates were three static mechanical properties selected for this program to determine the effect of testing techniques on the measured values of these pneumatic tire properties. Of these three mechanical properties, the fore-aft stiffness property was affected the most by different testing techniques used to obtain it. Appreciable differences in the fore-aft spring rates occurred using increment loading techniques and continuous loading techniques. However, varying the fore-aft force loop size had the most significant effect on the values for fore-aft stiffness.

The most consistent and usable technique for determining a value for fore-aft stiffness was based on generating and recording a continuous full cycle force-deflection loop. The stiffness value was then determined by measuring the slope of the line connecting the end points of the loop. To achieve consistent stiffness values, it was necessary to closely monitor operating conditions during the test, particularly the size of the force-deflection loop.

The dependence of lateral stiffness values on testing techniques followed the same trends as fore-aft stiffness values, except to a lesser degree. However, vertical stiffness values were found to be nearly independent of testing procedures and techniques. Due to a characteristic initial "soft" portion in

the vertical load-deflection curve, consistent values of vertical stiffness can only be obtained when its value is determined from a definition that by-passes the initial nonlinear portion of the force-deflection curve.

INTRODUCTION

Engineers measure and evaluate static mechanical properties of pneumatic tires for various reasons. Often the numerical values of these properties are exchanged among many engineering groups. This flow is an admirable exchange of technical knowledge and an economic use of time and effort. However, the indiscriminant use of such information can be unwise if these numerical values are not measured and interpreted consistently from one source to another. Thus, there is a definite need to investigate the effects of testing procedures and techniques on the static mechanical properties of pneumatic tires. Also, if it is evident that some properties are highly susceptible to testing techniques, it is possible that guidelines could be established for such measurements.

The general purpose of the test program discussed here was to systematically investigate the effects of testing techniques on three important static mechanical properties of pneumatic tires. These effects were to be studied on both scaled model aircraft tires as well as full size tires. In addition, it was hoped that this work would be useful in establishing criteria for measuring those properties that are highly influenced by testing techniques.

The static mechanical properties chosen for this study were vertical, lateral, and fore-aft spring rates. Each of these properties was to be measured and evaluated by various techniques and their results compared with one another. The techniques were to be varied according to the numerous methods used in the past by various testing groups.

The research group concerned with this program has been actively involved

in establishing structural modeling laws of pneumatic tires [1]. Some validity has been established for these laws by showing favorable correlation between some mechanical properties of prototype and model aircraft tires constructed according to the modeling laws. These model aircraft tires are used in this investigation as well as a variety of full size automobile and aircraft tires.

SYMBOLS

English Letters

D - tire diameter

F_x - tire fore-aft force

F_{xm} - maximum tire fore-aft force

F_y - tire lateral force

F_{ym} - maximum tire lateral force

F_z - tire vertical force

F_{zm} - maximum tire vertical force

k_x - tire fore-aft elastic stiffness

k_y - tire lateral elastic stiffness

k_z - tire vertical elastic stiffness

p_o - tire inflation pressure

x,y,z - tire coordinate directions (see Figure 1)

Greek Letters

δ_x - tire fore-aft deflection

δ_{xm} - maximum tire fore-aft deflection

δ_y - tire lateral deflection

δ_{ym} - maximum tire lateral deflection

δ_z - tire vertical deflection

δ_{zm} - maximum tire vertical deflection

TEST PROCEDURES AND RESULTS

The two coordinate system used in this work is shown in Figure 1. The mechanical properties discussed are described in terms of these coordinates. The x-direction is referred to as the fore-aft direction, the y-direction as the lateral direction, and the z-direction as the vertical direction.

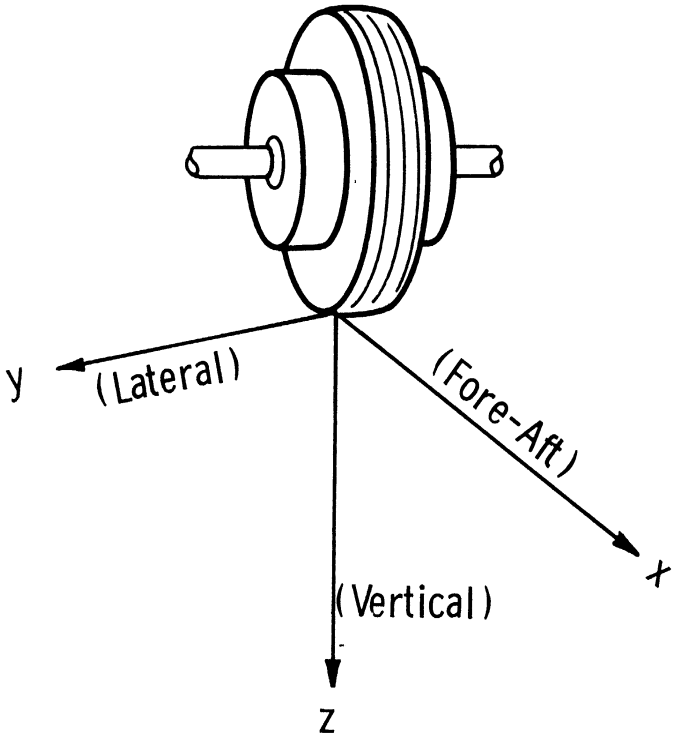

Figure 1. Tire coordinate directions.

The stiffnesses or spring rates in these directions are defined in terms of the ratio of applied force to resulting deflection. The fore-aft stiffness k_x is defined in terms of the fore-aft load F_x and the corresponding deflection δ_x obtained when a stationary time is first inflated and loaded vertically and then subjected to a varying fore-aft load. The lateral stiffness k_y is defined in terms of the lateral load F_y and the corresponding deflection δ_y obtained

when a stationary tire is first inflated and loaded vertically and then subjected to a varying lateral load. The vertical stiffness k_z is defined in terms of the vertical load F_z and the corresponding deflection δ_z obtained after a stationary tire is first inflated and then subjected to a varying vertical load.

Data necessary to investigate these properties were collected for both model and full size tires. The model aircraft tires were built according to the modeling laws and procedures discussed by Clark, Dodge, Lackey, and Nybakken [1]. The model tires used in these tests were scaled from 40 x 12-14 PR Type VII and 49 x 17-26 PR Type VII aircraft tires. The full size tires ranged from a foreign made 155 mm x 15 radial passenger car tire to a 24 x 7.7-10 PR Type VII aircraft tire.

Fore-Aft Stiffness

The test apparatus used to obtain fore-aft data for the model tires is shown in Figure 2. This apparatus is a revision of the Static Testing Device described in [1]. Its basic structure consists of a tire holding yoke attached to a counterweighted 90-degree elbow arm which in turn is attached to a fixed base through a steel pointed hinge. The yoke assembly is loaded vertically with dead weights, causing the tire to bear against a movable steel bearing plate. This plate is supported by three ball bearings rolling in steel guides. The bearing plate has a high friction surface bonded to it to minimize tire slippage. The tire was positively locked in the yoke assembly to minimize

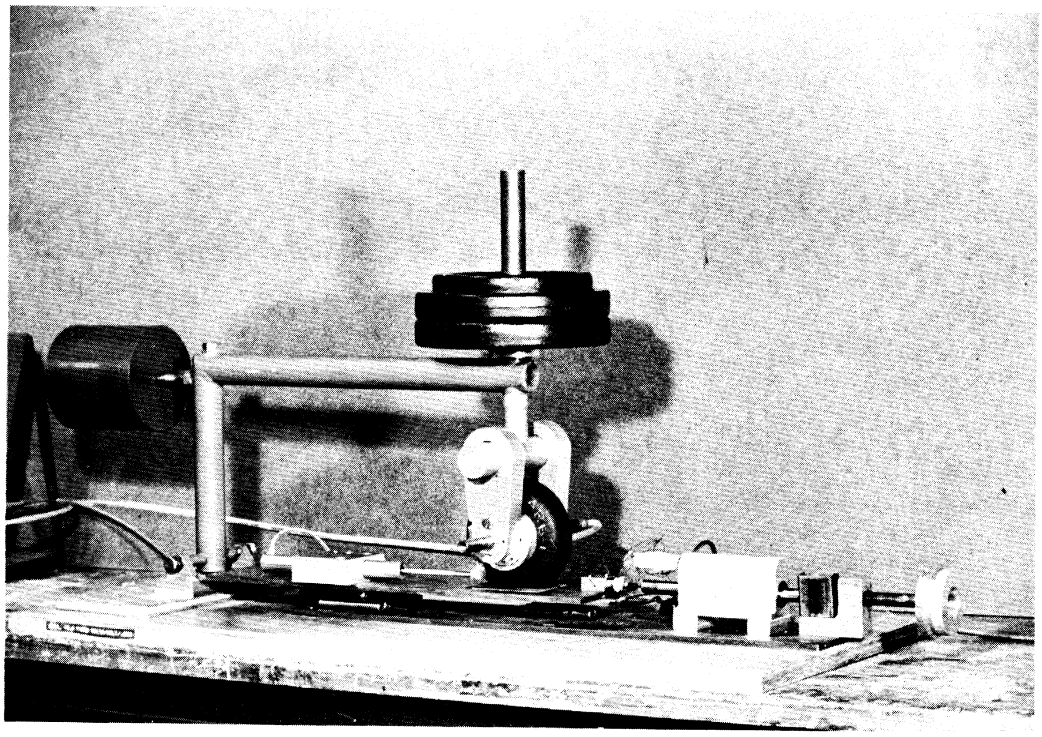

Figure 2. Photograph of fore-aft test apparatus for model tires.

wheel windup during the fore-aft tests. The three ball bearing supports had low friction characteristics and the effective friction coefficient of the total apparatus was 0.0138. This friction coefficient also held for the lateral tests.

Fore-aft data for the model tires were generally obtained by inflating the tire to a prescribed internal pressure and loading the tire vertically with a prescribed load. A varying fore-aft load was applied to the bearing plate through the screw assembly. Force was monitored by a calibrated force transducer located between the screw assembly and the bearing plate. Displacement was monitored by a Linear Variable Differential Transformer located between the yoke and the bearing plate. The placement of the LVDT is important, especially in fore-aft stiffness tests where the spring rate of the tire is high. The spring rate of the tire in the fore-aft direction can easily be of the same

order as the support structure. Measurement of the true tire deflection requires the relative displacement of the wheel hub and tne bearing plate. Because of the positive locking procedures used in these tests, wheel windup was found to be negligible. Thus, the relative displacement between the wheel yoke and the bearing plate was used as the measure of tire deflection. The output signals of both transducers were amplified througn carrier preamplifiers and recorded on a x-y plotter to give a force-deflection record.

The test apparatus used to obtain fore-aft stiffness data for the full size tires is shown in Figure 3. The apparatus is a modification of a Riehle

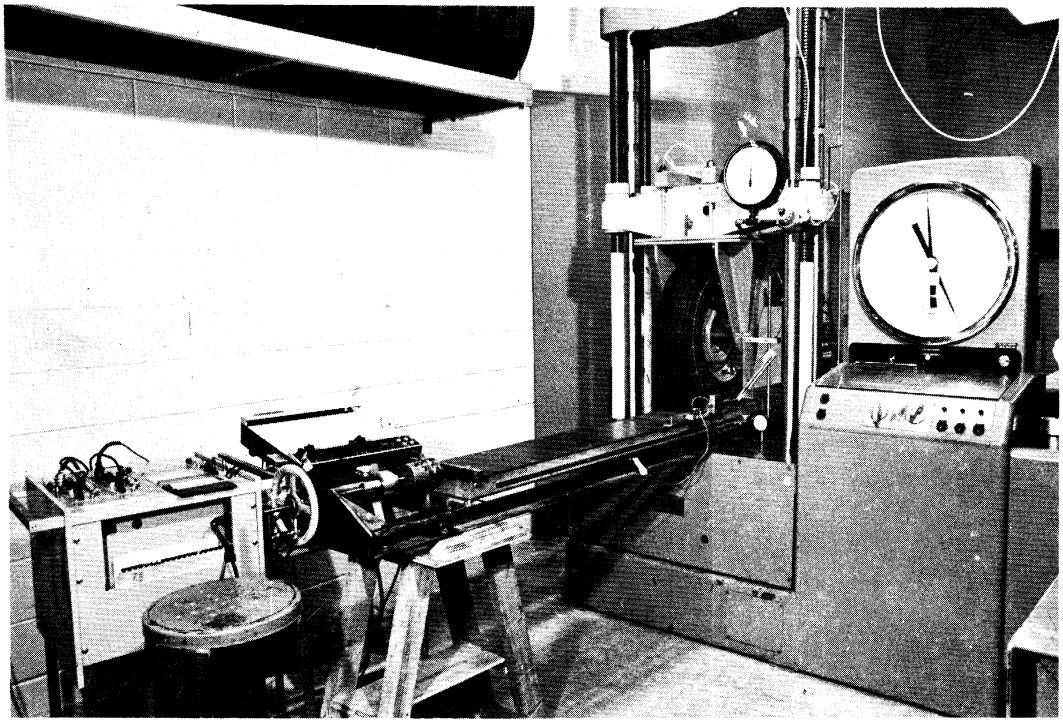

Figure 3. Photograph of fore-aft test apparatus for full size tires.

Tensile Test Machine into a slow-rolling flat plank machine. The wheel is bolted to the axle, which is rigidly bolted to the yoke which is bolted to the loading head of the testing machine. The tire is loaded vertically through

the loading mechanism of the machine, causing the tire to bear against a movable flat plank. The top surface of the plank directly under the tire has a number 80 grit sanding belt bonded to it. The plank is supported by low friction rollers located directly under the loading area and is guided by ball bearings located along the length of the plank and running against a stationary steel angle guide. This plank arrangement results in low friction characteristics and has an effective friction coefficient of 0.006, considerably lower than the model tire system. The fore-aft load is applied to the end of the movable plank. A tension-compression load cell is placed between the loading screw and the plank. The displacement is measured with the same LVDT used in the model tests. Again the LVDT is located between the plank and the yoke, since wheel-axle windup was negligible with the rigid system used in these tests.

The fore-aft data for the full size tires were obtained in the same manner as the data for the model tires. One minor difference was caused by the nature of the two loading systems. The model tires were always operating under a fixed vertical load while the full size tires were always operating under fixed vertical deflection. However, the basic operation of the full size test apparatus was very similar to that used for the model tires.

A brief description of the model and full size tires used in these tests is given in Table I. The A-series model tires are scale models of 40 x 12-14 PR Type VII aircraft tires with a scale factor of 8.65 and the B-series model tires are scale models of 49 x 17-26 PR Type VII aircraft tires with a scale factor of 12. Each model tire had been run through a break-in period before

TABLE I

TIRE DESCRIPTIONS

Model Tires	
A24	2-ply bias model of 40 x 12-14 PR Type VII, crown angle 39°, 840/2 Nylon, 10 EPI
A23P	2-ply bias model of 40 x 12-14 PR Type VII, crown angle 36°, 840/2 Nylon, 10 EPI
B21	2-ply bias model of 49 x 17-26 PR Type VII, crown angle 42°, 840/2 Nylon, 28 EPI
B23	2-ply bias model of 49 x 17-26 PR Type VII, crown angle 42°, 840/2 Nylon, 28 EPI
B26	2-ply bias model of 49 x 17-26 PR Type VII, crown angle 41°, 840/2 Nylon, 10 EPI
B29'	2-ply bias model of 49 x 17-26 PR Type VII, crown angle 34°, 840/2 Nylon, 10 EPI
Full Size Tires	
1	24 x 7.7-10 PR Type VII, aircraft
2	8.00 x 14, 4-ply bias, automobile
3	7.50 x 14, 2-ply bias, automobile
4	7.50 x 14, 4-ply radial, foreign, automobile
5	5.90 x 15, 4-ply bias, foreign, automobile
6	155 x 15, radial, foreign, automobile
7	215 R 15, radial, automobile
8	7.50 x 14-8 PR Type III, aircraft
9	H78-15, belted bias, automobile
10	G78-15, belted bias, smooth tread, automobile
10M	G78-15, belted bias, smooth tread, automobile

being used in any test. Most of the full size tires had not gone through such a break-in period.

The operating conditions for the model and full size tires are given in Table II. For the model tires, the vertical force is prescribed while the vertical deflection is prescribed for the full size tires. The full size tire vertical deflections were obtained by loading the tires to the approximate rated load as specified by the Tire and Rim Association and then measuring the

TABLE II

TIRE OPERATING CONDITIONS

Tire	D (in.)	p_o (psi)	F_z (lb)	δ_z (in.)	F_{xm} (lb)	F_{ym} (lb)
A24	4.55	20	41.6	.327*	± 6	± 5
A23P	4.55	20	41.6	.319*	± 6	± 5
B21	4.00	25	31.6	.211*	± 6	± 5
B23	4.00	25	31.6	.216*	± 6	± 5
B26	4.00	25	31.6	.224*	± 6	± 6
B29'	4.00	25	31.6	.197*	± 6	± 5
1	23.7	85	4800*	1.90	---	---
2	25.1	24	1175*	1.125	±225	±200
3	27.9	24	1085*	1.00	±275	±225
4	26.9	24	1085*	1.34	±250	±200
5	25.8	20	770*	1.00	±200	±150
6	24.5	20	770*	1.25	±175	±150
7	28.2	24	1510*	1.75	±300	±250
8	27.5	87	5400*	1.70	±500	±500
9	28.4	24	1510*	1.24	±300	±250
10	27.7	24	1380*	1.00	±250	±230
10M	27.7	24	1380*	1.00	±250	±230

*Approximate values.

deflections. Also shown in Table II are the maximum and minimum fore-aft load F_{xm} and lateral load F_{ym} used for most of the tests.

Eight different testing techniques were used to obtain fore-aft stiffness data. Each of these techniques is described below by number and the results from their use are discussed. All of the tires listed in Tables I and II were not subjected to all eight testing techniques. For tests 1-7, the model tires were run on number 220 grit silicon carbide sandpaper and the full size tires were run on number 80 grit sanding belt.

Test 1 - Increment loads, half cycle, slow loop.

The tire was pressurized and vertically loaded to the conditions given in

Table II. An increment of fore-aft load was applied to the system and held constant for one minute, at which time the resulting fore-aft deflection was recorded. The fore-aft load was then increased by the same increment and the procedure repeated. This incremental loading was continued until the fore-aft load had reached the maximum F_{xm} given in Table II. The fore-aft loads were then decreased in a similar manner until the fore-aft load returned to zero. The resulting force-deflection data were plotted and the fore-aft stiffness k_x determined by averaging the best straight line fits to the increasing and decreasing portions of the plots. These best fit straight lines were obtained "by eye." The fore-aft stiffness k_x was also determined by forming the ratio of the maximum fore-aft load F_{xm} and its resulting deflection δ_{xm} to obtain (F_{xm}/δ_{xm}). The waiting time of one minute between increments of load was a controlled attempt to allow the tire to reach equilibrium before recording the deflection. This test procedure, Test 1, is representative of those used by testing groups that only have the facilities for taking half-cycle, increment load data.

Test 2 - Increment loads, full cycle, slow loop.

This test procedure was identical to Test 1 except the load cycle was continued in both directions, thus generating a full cycle of fore-aft load-deflection data. The fore-aft spring constant k_x was determined by measuring the slope of the line joining the end points of the fore-deflection loop. This determination of k_x eliminates the observer's "eye" approximation used in Test 1. Again the maximum and minimum fore-aft forces are those given in Table II.

Test 3 - Increment loads, full cycle, fast loop.

This test was a repeat of Test 2 except the loads were held constant for 15 seconds instead of one minute. This procedure was a controlled attempt to determine time effects on increment load tests.

Test 4 - Continuous loads, slow loop.

This test was also a repeat of Test 2 except the loads were continuously applied from zero to the maximum F_{xm}, back through zero to the minimum F_{xm} and back to zero. However, the test was not stopped after one cycle, but continued for several loops. In these tests, the loops were continued until the generated loop "homed in" on a single path. In most cases the single path was generated on the second or third cycle. The time for one complete cycle was approximately one minute. The value of the fore-aft stiffness k_x was again determined by measuring the slope on the line joining the end points of the force-deflection loop. This test procedure, Test 4, is representative of those testing groups that have the capabilities of obtaining a full loop of force-deflection through a continuous loading system.

Test 5 - Continuous loads, fast loop.

This test was identical to Test 4 except the load cycle was completed in approximately 10 seconds instead of one minute. This test was included to determine time effects for continuous loading conditions.

Test 6 - Continuous loads, slow loop, plate deflection.

This test was also identical to Test 4 except deflections were measured between the fixed base and the bearing plate. This test was included to illustrate possible errors when the wheel, yoke and support mechanism are assumed rigid.

Test 7 - Continuous loads, varying force loop size.

This test was basically tne same as Test 4 with a complete loop generated in approximately 20 seconds. In this test, the maximum fore-aft force applied F_{xm} was varied over a range of values. This procedure resulted in 4 or 5 different size force-deflection loops. The fore-aft stiffness k_x was determined using the Test 4 procedure of connecting the end points.

Test 8 - Continuous loads, varying contact surface conditions.

This test was also basically the same as Test 4. The high friction surface test was the same as in Test 4. After this test the tire was thoroughly cleaned. The high friction surface was removed from the bearing plate and the metal surface of the plate was cleaned thoroughly. The test procedure described in Test 4 was then repeated. Next an oiled surface and then a dirty surface (oil mixed with grit and sand) were tested in the same manner. Finally, the plate and tire were thoroughly cleaned and the tire bonded to the bearing plate with methyl-2 cyanoacrylate. At the instant of bonding, the tire was maintained at the prescribed operating conditions given in Table II. The test procedure was then repeated, again using the force loop size given in Table II. Due to the possibility of tire damage during the unbonding, the tires used in this test, Test 8, were different than the tires used previously in Tests 1-7.

The results of Tests 1-8 are summarized in Table III. The friction forces of the testing apparatus have not been taken into account in arriving at the fore-aft stiffnesses given in this table. The results given in the table indicate that all tires, both model and full size, have the same general trends. However, the different in stiffness values between Test 5 and the preceding

TABLE III

SUMMARY OF STATIC FORE-AFT STIFFNESS

k_x(lb/in.)

Test / Tires	1 $\frac{F_{xm}}{\delta_{xm}}$	1 k_x	2 k_x	3 k_x	4 k_x	5 k_x	6 k_x	7 ± Force Loop Size / Value of k_x					8				
								± 2	± 4	± 6	± 8	± 10	High Friction	Clean Metal	Oil	Oil + Grit	Bonded
A24	319	354	346	348	376	381	247	457	402	377	368	355	---	---	---	---	---
A23P	---	---	---	---	---	---	---	---	---	---	---	---	326	328	---	335	384
B21	320	354	337	370	396	413	---	506	441	420	395	369	---	---	---	---	---
B23	---	---	---	---	---	---	---	---	---	---	---	---	365	349	---	357	466
B26	300	342	317	340	351	363	---	424	384	364	344	333	---	---	---	---	---
B29'	326	343	336	362	378	388	---	454	412	393	373	349	---	---	---	---	---
2	2620	2880	2880	3040	3370	4140	2530	± 50 6190	± 100 5000	± 150 4470	± 200 4220	± 225 4160	---	---	---	---	---
3	2990	3380	3040	3240	3440	3660	---	± 50 4940	± 100 4360	± 150 4100	± 200 3800	± 250 3660	---	---	---	---	---
4	1680	1750	1690	1780	1780	1810	---	± 50 2020	± 100 2020	± 150 1460	± 200 1870	± 250 1840	---	---	---	---	---
5	3020	2680	3130	3300	3690	3790	---	± 50 5100	± 100 4850	± 150 4070	± 200 3730	---	---	---	---	---	---
6	1380	1410	1410	1470	1530	1560	---	± 50 1720	± 100 1650	± 150 1560	± 175 1560	---	---	---	---	---	---
7	1400	1320	1460	1550	1630	1630	---	± 50 2160	± 100 1820	± 150 1770	± 200 1690	± 300 1630	---	---	---	---	---
8	5210	5700	5860	6190	6670	6800	---	± 100 9300	± 200 7950	± 300 7580	± 400 6930	± 500 6810	---	---	---	---	---
9	3410	3720	3460	3610	3820	3950	---	± 50 5930	± 100 4900	± 150 4480	± 200 4210	± 300 3920	---	---	---	---	---
10	4170	3930	3980	4000	4130	4170	---	± 50 5260	---	± 150 4690	± 200 4520	± 250 4480	---	---	---	---	---
10M	---	---	---	---	---	---	---	---	---	---	---	---	4960	4930	4910	4730	5060

four tests is somewhat greater for Tire 2 than any other tire.

A number of specific observations can be made concerning the fore-aft stiffness tests:

(a) The values of k_x determined from increment load tests, with the exception of Tire 2, ranged from 5-15% lower than those determined from continuous load tests. See the results for Tests 1-5.

(b) The values of k_x determined from full cycle increment load data from model tires were 2-7% less than those determined from half cycle increment load data. On the other hand, the full cycle values for the full size tires ranged from ± 10% of the half cycle values. A further indication of the differences encountered in determining k_x from half cycle and full cycle increment data is shown in Figure 4. This figure presents typical increment load force-deflection plots for a model tire and a full size tire. The friction force is indicated by the bar in the figure, but has not been subtracted from the data presented. It is apparent from these plots that the various interpretations of k_x mentioned previously can lead to different values of k_x.

(c) The slope of the line from the origin to the maximum force-deflection point, F_{xm}/δ_{xm}, was usually lower than either of the values of k_x determined from the increment load techniques on Tests 1 or 2.

(d) The values of k_x determined from the fast increment loading loops were 0-9% higher than those determined from the slower increment loading loops. See the results of Tests 2 and 3.

(e) The values of k_x determined from the faster continuous loading loops, with the exception of Tire 2, were 0-6% higher than those determined from the

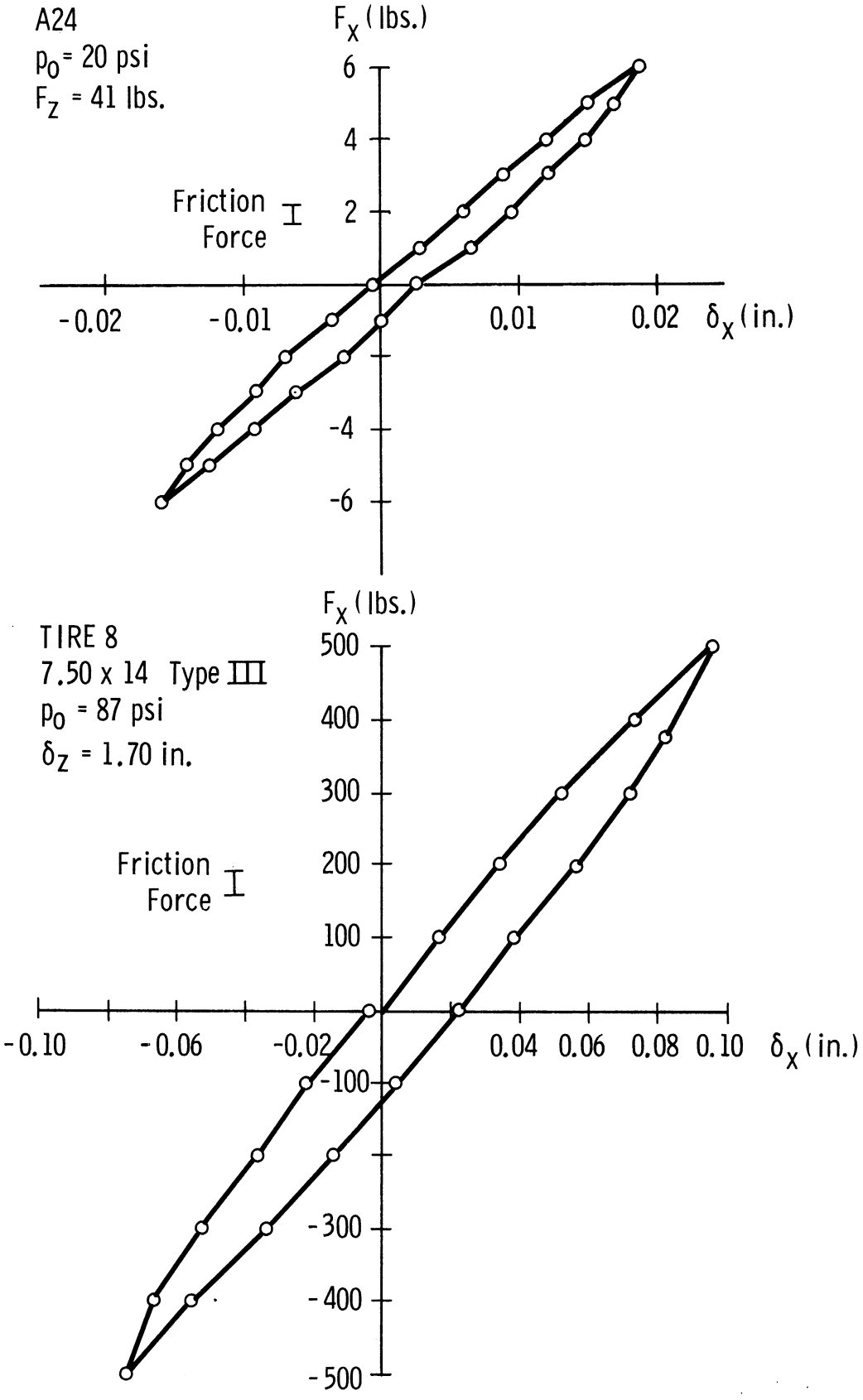

Figure 4. Typical fore-aft, increment load, force-deflection plots for model and full size tires.

slower continuous loading loops. See the results of Tests 4 and 5.

(f) The values of k_x determined by measuring the plate deflection and assuming it to be equal to the tire deflection were 25-40% lower than those obtained using the relative displacement between yoke and plate. See tne results of Tests 5 and 6. This result is a clear indication of the role of yoke and support deflections in measuring the relatively stiff fore-aft spring rate of a tire.

(g) The values of k_x decreased from 12-50% as the force loop size was increased from a small value to a maximum value. See the results of Test 7. A further indication of this significant difference is clearly illustrated in Figures 5 and 6. Figure 5 shows a typical composite force-deflection plot for two different loop sizes for a model tire. Figure 6 shows the same type of plot for a full size tire. Again the friction force is indicated on the two figures, but is not subtracted from the data shown.

(h) The values of k_x varied less than 5% for the tests conducted under various surface conditions. However, when the model tires were bonded to the surface, the value of k_x increased 16-23% while the full size tire value increased only 5%. It is not clearly understood why the increase is so different between the model tires and the full size tire. The reason may be in the difference between the contact patch geometries. The model tire has a typical aircraft tire geometry, with circumferential grooves and little rubber buildup at the tire shoulders. When loaded to 30-33% vertical deflection, the tire has a rounded contact patch [1]. The full size tire is a typical automotive tire with pronounced shoulders but with no tread pattern. The resulting

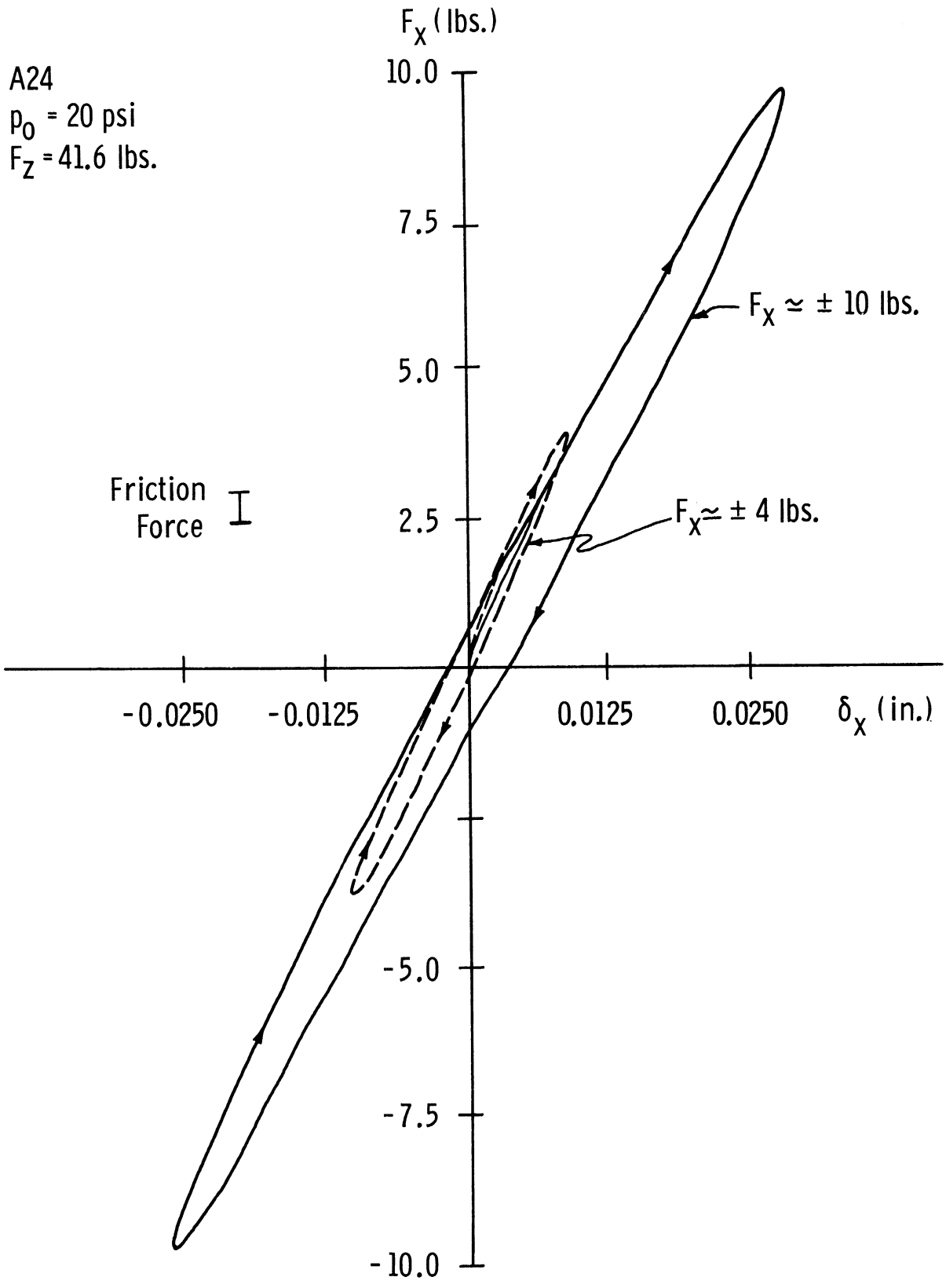

Figure 5. Fore-aft force-deflection loops illustrating effect of loop size for a model tire.

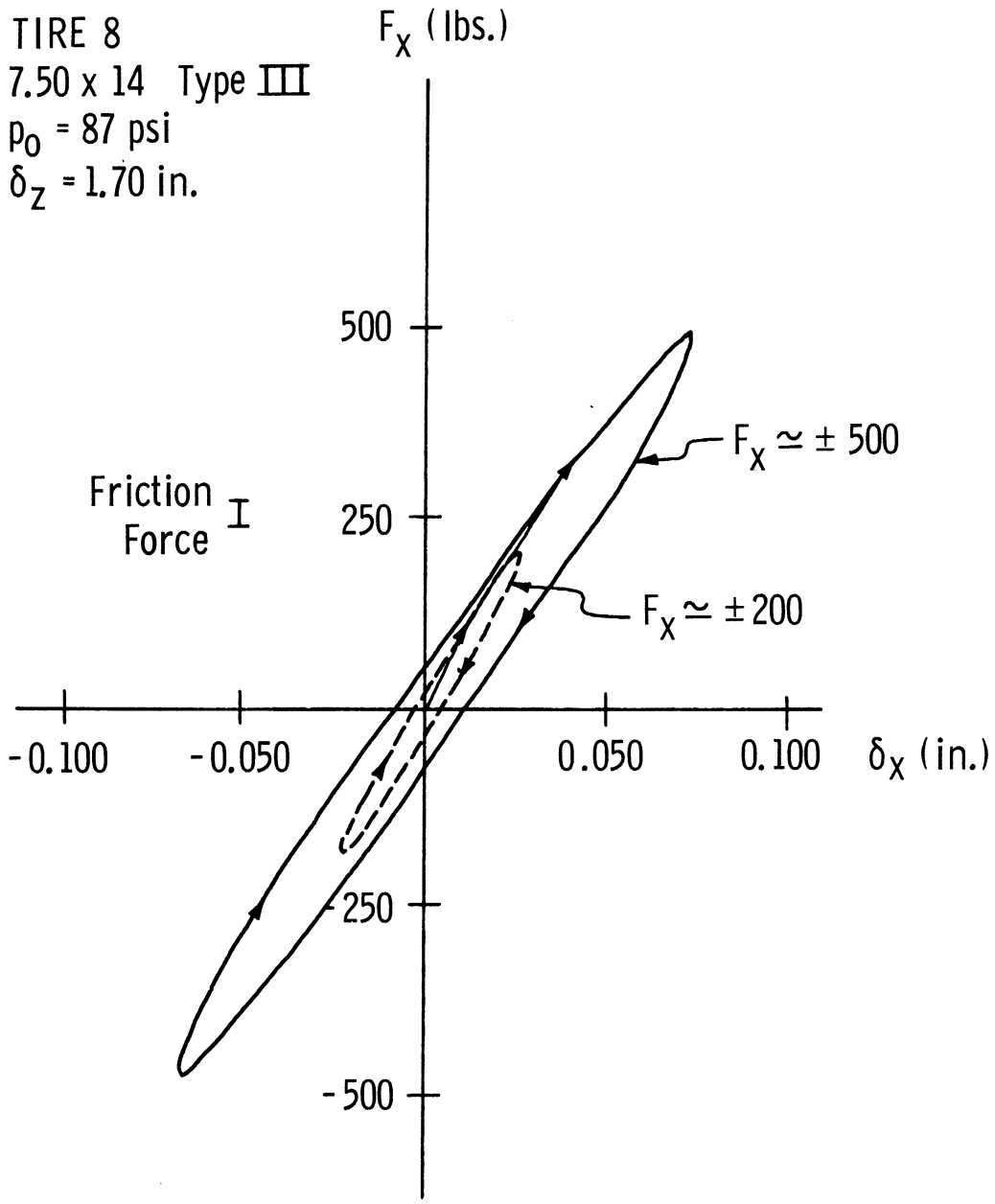

Figure 6. Fore-aft force-deflection loops illustrating effect of loop size for a full size tire.

contact patch is almost a perfect rectangle. These contact patch geometry differences may cause different deformation patterns when the tire is bonded to the plate and distorted in the fore-aft direction. The fact that the fore-aft stiffness does increase with bonding may have two possible explanations. The first possible reason may be based on the restraining of the tire contact patch from stretching when the tire is bonded. The net deflection for a given load is less, resulting in a higher spring rate. The second reason is based on the restraining of local slip in those regions of the contact patch where the vertical pressure distribution is small. This restriction on the bonded tire again results in a smaller deflection and a higher spring rate.

From the results and observations discussed above, it seems there are several important suggestions to be made in regards to obtaining and interpreting static fore-aft mechanical properties of pneumatic tires. First, if k_x is measured by loading a locked tire against a movable plate which in turn is loaded in the fore-aft direction, care should be taken to measure relative deflection between the plate and the wheel and not between the ground and the plate. Even using apparatus that appears to be fairly rigid can lead to substantial errors in deflection measurement, as the results of Test 6 illustrate.

Secondly, a crude estimate of a tire's fore-aft stiffness can be obtained by applying a single fore-aft load and measuring the resulting deflection. The ratio of these two values gives a reasonable estimate for k_x. In general, this estimate will be less than the true value.

Finally, it might be recommended that the most consistent and useful method for measuring k_x is with a system that allows full cycle, continuous

load loops to be generated and recorded in the form of x-y plots. There are several reasons for this recommendation. First, a consistent interpretation of the value for k_x is possible if a full force-deflection loop is available. This interpretation specifically defines k_x as the slope of the line joining the end points of the loop. This method eliminates the need for best fits or other approximations. However, as the discussion above indicates, a value of k_x can only be used and interpreted in a consistent manner if the operating conditions for which the value was measured are well monitored and clearly indicated. In particular, the inflation pressure, the vertical load, and the fore-aft load loop size should be clearly defined. The inflation pressure and vertical load can be fixed in relation to an easily obtainable rated condition. However, no such specification exists for the fore-aft loop size. The effect of fore-aft loop size on the measured value of the fore-aft stiffness can be clearly seen in Figure 7. Figure 7 is a composite plot of k_x as a function of varying force loop size in dimensionless form for all the tires tested in Test 7. The results shown in Figure 7 indicate the size of the fore-aft loading loop must be taken into account when comparing fore-aft stiffnesses of different tires. A standard loop size might be defined as a fixed percentage of the vertical load or the vertical deflection.

The continuous loading full loop also has the advantage of displaying unusual and, usually, unwanted characteristics of the load-deflection data. Figures 8, 9, and 10 are examples of force-deflection loops with undesirable features. Figure 8 shows a fore-aft force-deflection loop where slippage has occurred between tire and plate. Comparing Figure 8 with the usual loops in

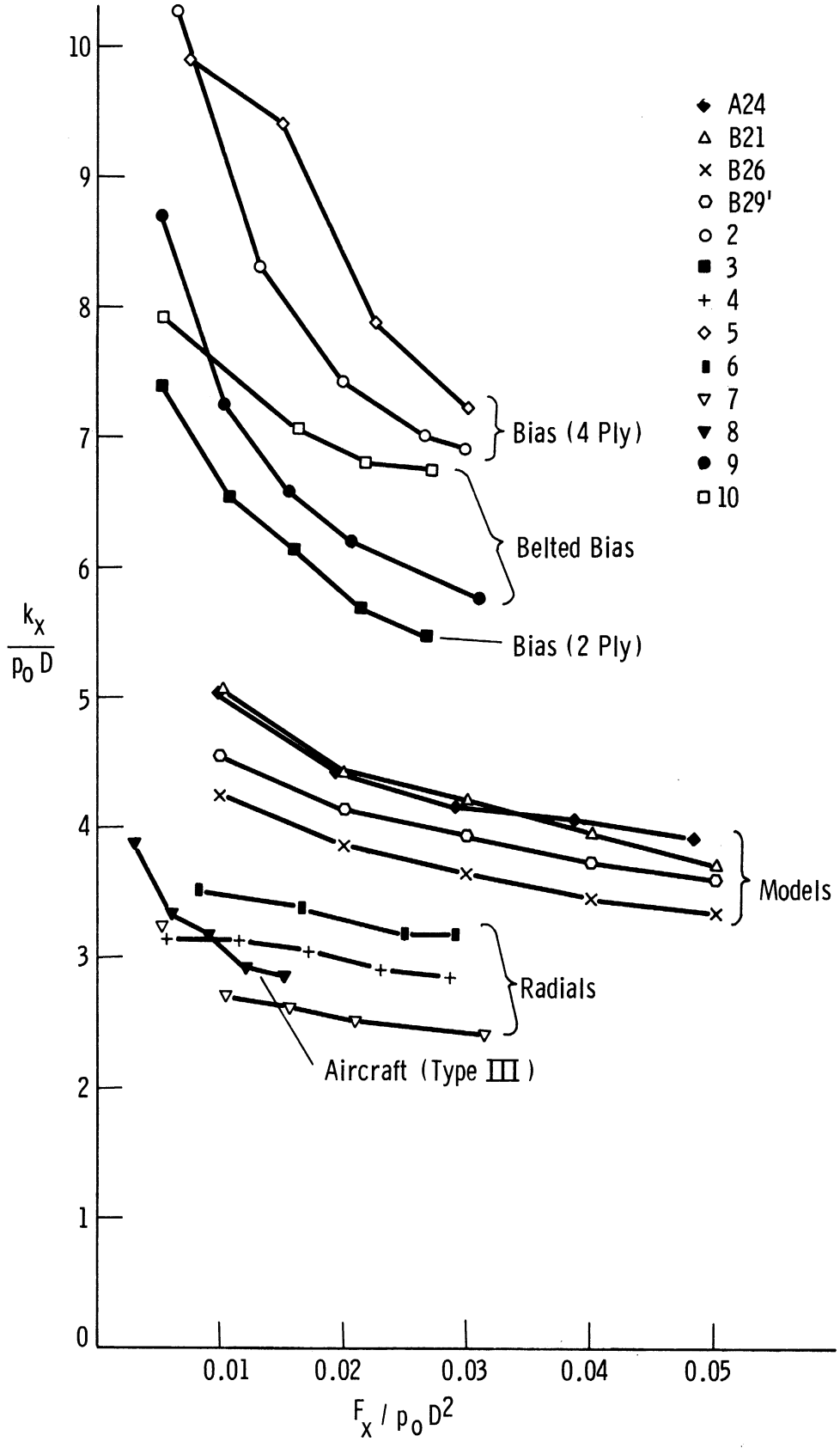

Figure 7. Dimensionless plot of fore-aft stiffness versus loop size for all tires.

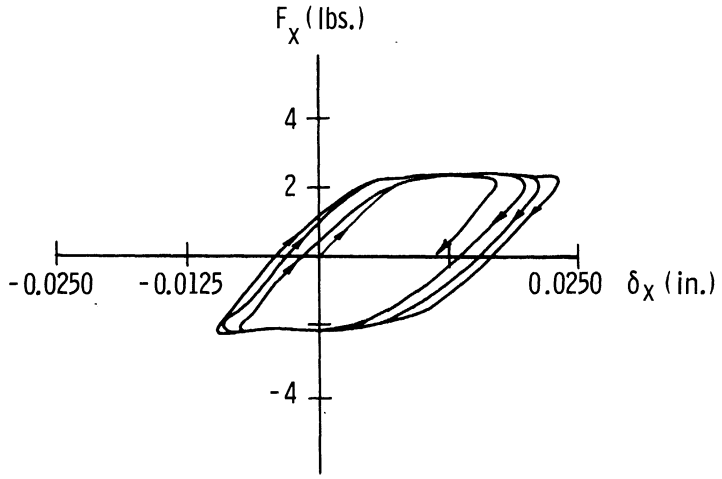

Figure 8. Fore-aft force-deflection loop illustrating tire slippage during testing of a model tire.

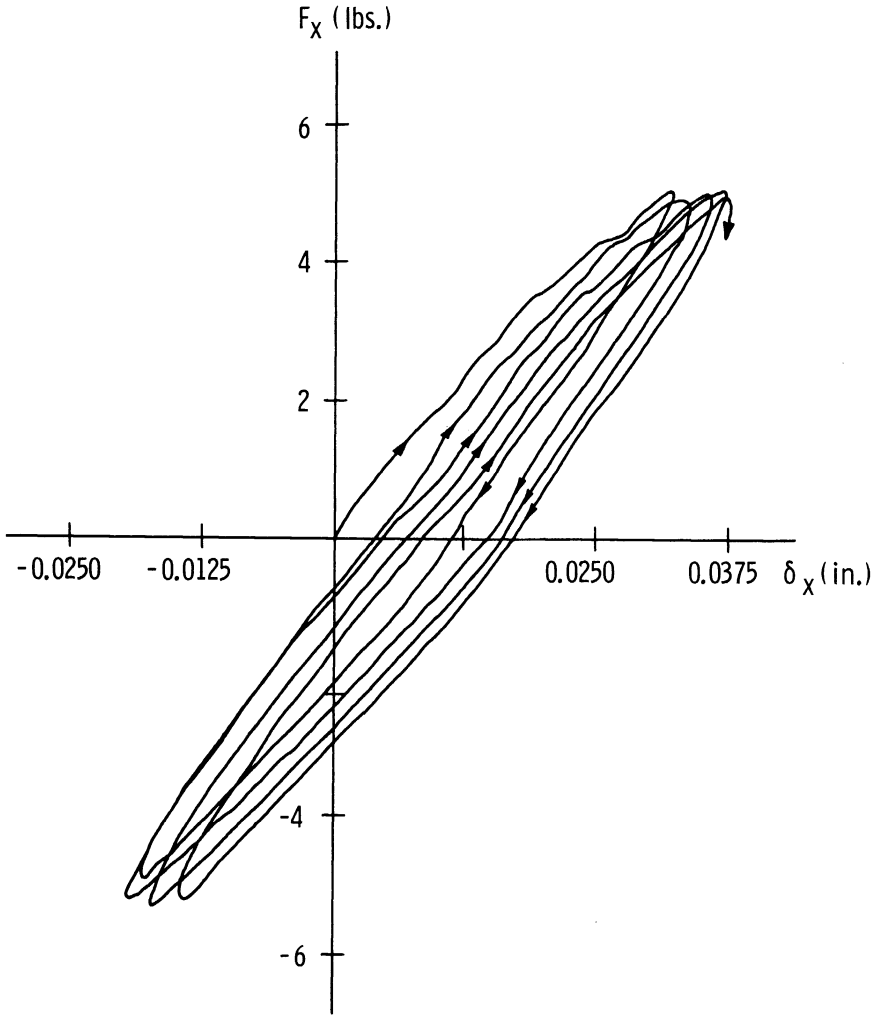

Figure 9. Fore-aft force-deflection loop illustrating small, unidirectional slippage during testing of a model tire.

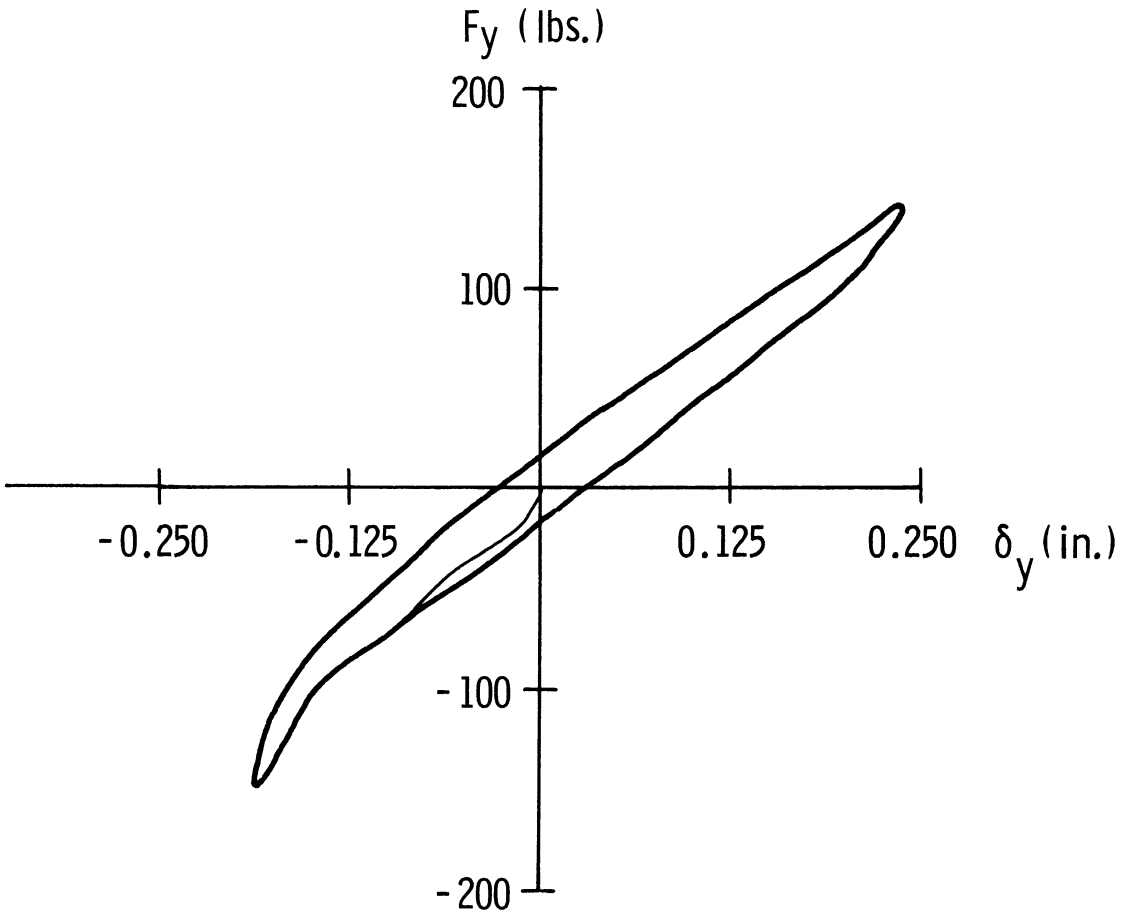

Figure 10. Lateral force-deflection loop illustrating dog leg type loop generated during testing of a full size tire.

Figure 5 and 6 illustrates the large flat portions at the high loads where large deflections are occurring with no increase in load. Also, the absence of a homing in on a single loop indicates that more slippage has occurred in one direction than the other. Figure 9 illustrates this same effect, even though the slippage is not obvious. In this case, the lack of a homing in on a single path is caused by improper locking of the wheel in the yoke. Even though the force continues to rise with deflection, a slight slippage has occurred between the axle and the yoke. This slippage is unidirectional and results in the absence of a final, single loop. Figure 10 illustrates a dog-leg type feature of a force-deflection loop. In this case, the dog leg was generated by running the plate into an unnoticed obstruction. The obstruction acted like a stiff spring in series with tire at one end of the loop and caused the stiffer portion of the loop. Dog-leg loops can also be caused by measuring the deflection with respect to ground and having a support structure that is stiffer in one direction than the other. In this case the structure acts like a spring in series with the tire but with asymmetric force-deflection properties. The resulting force-deflection loop will have a dog leg at the origin. Although the undesirable characteristics of a fore-aft test might be obvious when one looks at the resulting force-deflection loop, these characteristics might go unnoticed in half cycle or increment loading tests or at least go unnoticed until the data are plotted after the test. The simultaneous x-y recording of the force and the deflection during the actual test can indicate test difficulties immediately and obviously, especially when continuous loading, full loops are generated.

Lateral Stiffness

The testing apparatus used to obtain lateral stiffness data for the model and full size tires was the same as that used in obtaining the fore-aft data. The only change in the model and full size equipment was to position the tire holding yoke such that the tire was 90° from its orientation used in the fore-aft test. Figures 11 and 12 show the model and full size lateral testing apparatus. This arrangement provided a lateral force and deflection on the tire as load was applied through the screw mechanisms of each apparatus. The forces and deflections were measured in the same manner as in the fore-aft tests. The same eight test techniques described for the fore-aft tests were used for the lateral tests. The same tires and operating conditions listed in Table II were also used, except for the standard lateral force magnitudes F_{ym}, which are also listed in Table II.

The results of the various lateral tests are summarized in Table IV. Again, friction forces of the testing apparatus have not been taken into account for these values. Several observations can be made from these results:

(a) The values of lateral stiffness k_y determined from increment load tests were 5-15% less than those determined by continuous load tests. See the results of Tests 1-5. This result was very similar to that observed for fore-aft tests.

(b) The values of k_y for the model tires determined from full cycle increment load data were 6-10% greater than those determined from half cycle data. This result is in direct contrast to that observed for the fore-aft tests.

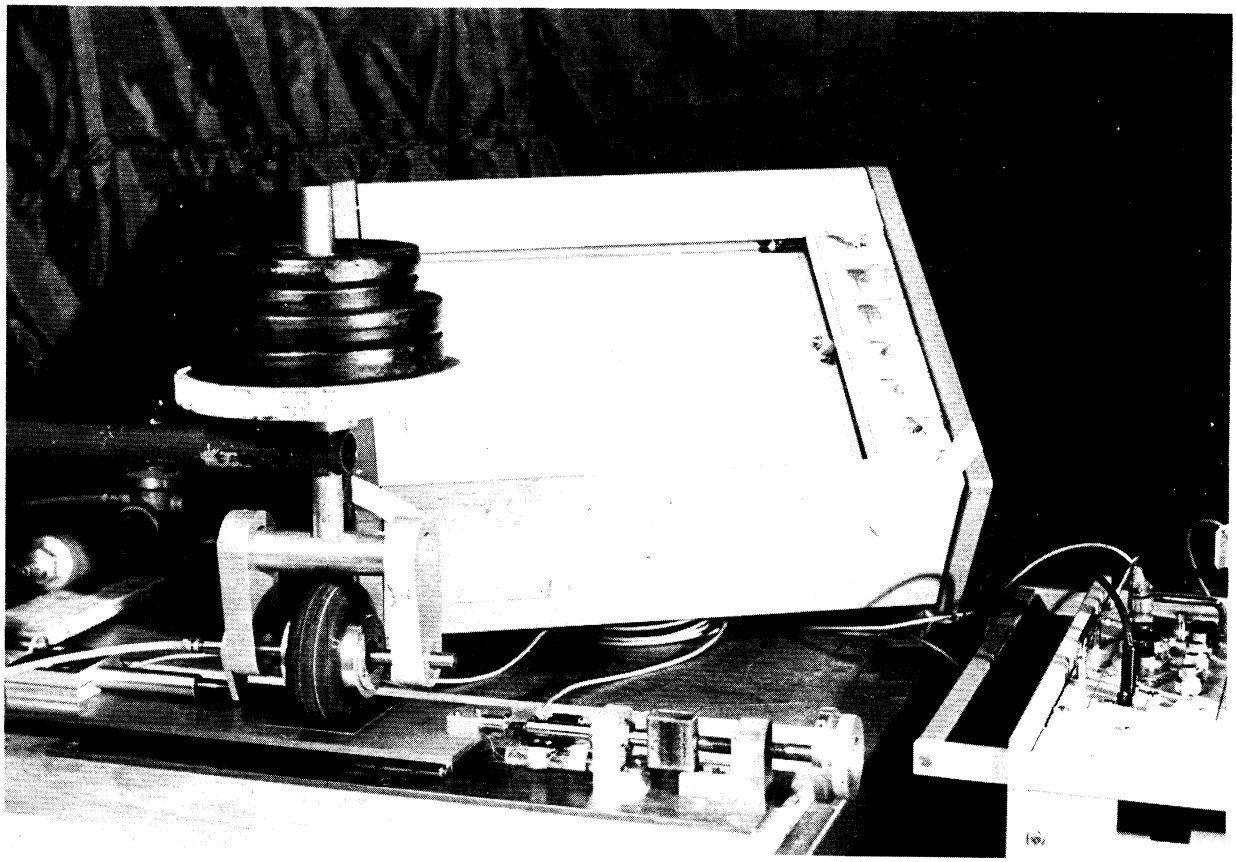

Figure 11. Photograph of lateral test apparatus for model tires.

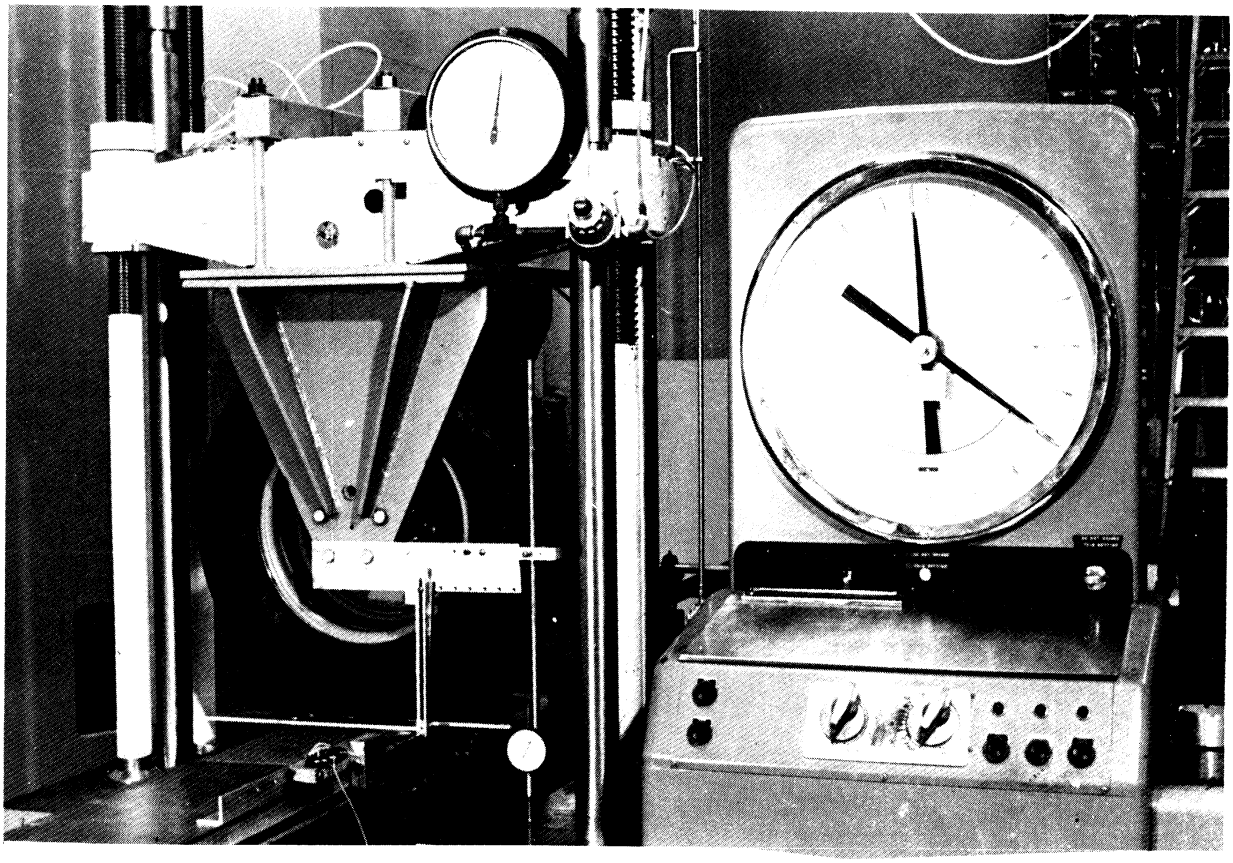

Figure 12. Photograph of lateral test apparatus for full size tires.

TABLE IV

SUMMARY OF STATIC LATERAL STIFFNESS

k_y(lb/in.)

Test / Tires	1 $\frac{F_{ym}}{\delta_{ym}}$	1 k_y	2 k_y	3 k_y	4 k_y	5 k_y	6 k_y	7 ± Force Loop Size / Value of k_y					8 High Friction	8 Clean Metal	8 Oil	8 Oil + Grit	8 Bonded
A24	78	73	80	84	85	85	---	± 2 95	± 4 85	± 6 83	± 8 80	---	---	---	---	---	---
A23P	---	---	---	---	---	---	---	---	---	---	---	---	80	80	---	---	90
B21	97	95	106	110	114	116	95	± 2 129	± 4 119	± 6 116	± 8 113	± 10 109	---	---	---	---	---
B23	---	---	---	---	---	---	---	---	---	---	---	---	116	114	---	116	125
B26	---	---	---	101	102	105	---	± 2 116	± 4 108	± 6 100	± 8 96	± 10 93	---	---	---	---	---
B29'	86	84	89	93	95	97	---	± 2 105	± 4 98	± 6 94	± 8 90	± 10 87	---	---	---	---	---
2	640	710	680	710	740	780	---	± 50 930	± 100 870	± 150 800	± 200 770	---	---	---	---	---	---
3	610	640	610	620	660	680	---	± 50 810	± 100 740	± 150 690	± 200 690	± 225 660	---	---	---	---	---
4	590	580	560	560	580	590	---	± 50 680	± 100 620	± 150 590	± 200 590	---	---	---	---	---	---
5	560	600	540	610	600	620	530	± 50 710	± 75 660	± 100 660	± 150 620	---	---	---	---	---	---
7	500	500	520	530	550	560	---	± 50 680	± 100 620	± 150 600	± 200 570	± 250 560	---	---	---	---	---
8	1800	1740	1850	2040	2010	2040	---	± 100 2390	± 200 2200	± 300 2180	± 400 2120	± 500 2070	---	---	---	---	---
9	670	670	680	690	740	740	---	± 50 980	± 100 850	± 150 790	± 200 760	± 250 740	---	---	---	---	---
10	690	700	700	760	790	800	---	± 50 970	± 100 890	± 150 830	± 200 810	± 230 790	---	---	---	---	---

However, the full cycle values of k_y for the full size tires were within ± 10% of the half cycle values, as they were for the fore-aft tests. Figure 13 shows typical increment lateral load-deflection plots for a model and a full size tire. Again the friction force is indicated on the plot, but is not subtracted from the data. Again it is apparent that different values of k_y can be determined with different interpretations of the data.

(c) Unlike the fore-aft results, the ratio of F_{ym}/δ_{ym} was usually between the values of k_y determined for Tests 1 and 2.

(d) The values of k_y determined from fast increment loading loops were 0-11% greater than those determined from the slower increment loading loops. Again this result agrees with the fore-aft test results.

(e) The values of k_y determined from fast continuous loading loops were 0-5% greater than those determined from slower continuous loading loops. Again this result agrees with the fore-aft test results.

(f) The values of k_y determined by measuring plate deflection and assuming it to be tire deflection were 12-17% lower than those determined by measuring the relative displacement between plate and yoke. This result is lower than that obtained from the fore-aft tests and might be expected. Although the testing system has the same effective stiffness as before, the lateral stiffness of the tire is approximately 1/3 the fore-aft stiffness. Thus, the percentage of the total lateral deflection due to the structure is lower than in the case of the fore-aft deflection.

(g) The values of k_y decreased 13-24% as the force loop size was increased from a small prescribed value to a maximum size. This difference is

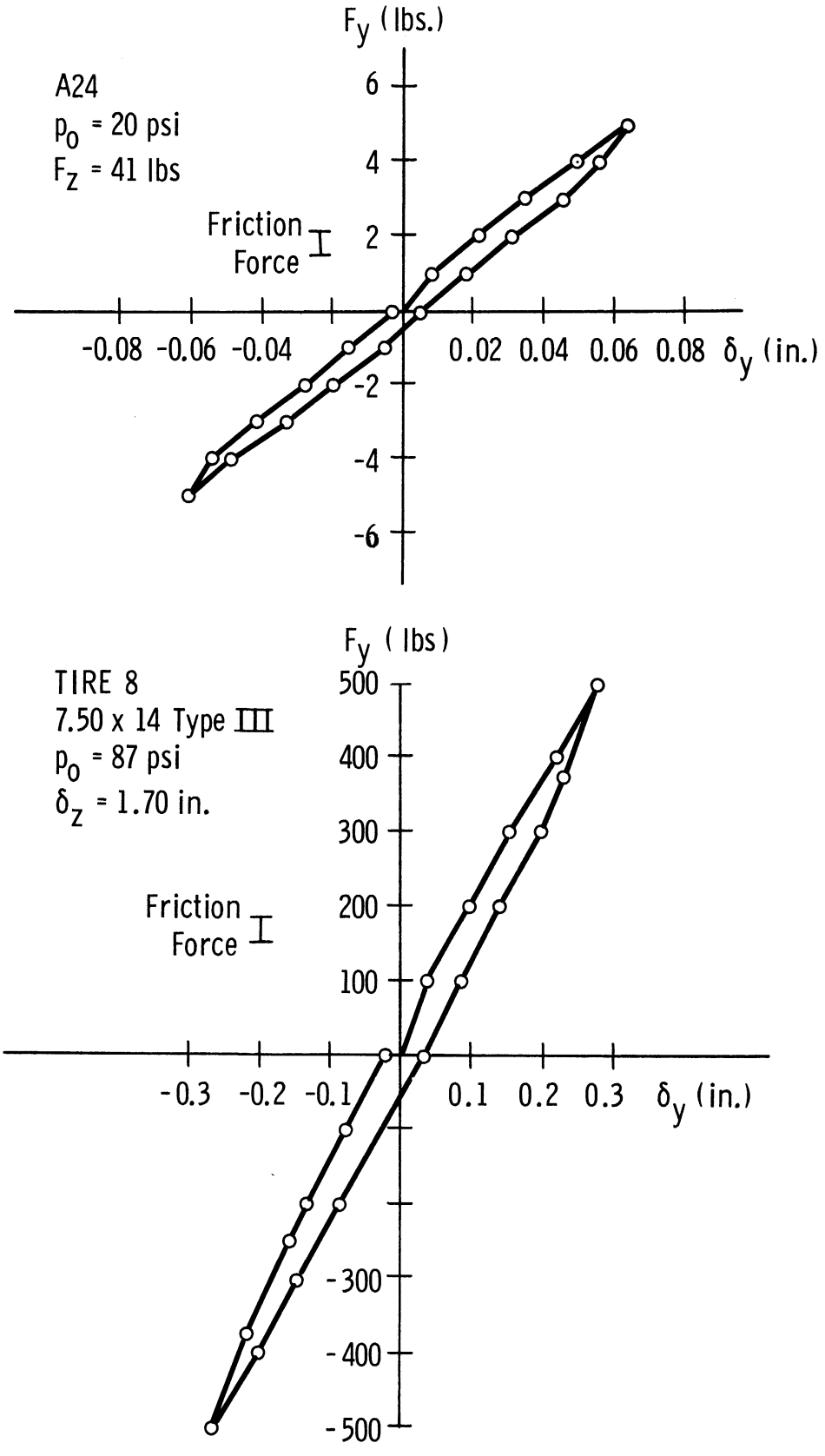

Figure 13. Typical lateral, increment load, force-deflection plots for model and full size tires.

clearly seen in Figures 14 and 15. Figure 14 is a typical composite force-deflection plot for two different size loops for a model tire. Figure 15 is a similar plot for a full size tire. A dimensionless plot of lateral stiffness versus lateral loop size for all the Test 7 results is shown in Figure 16.

(h) For the model tires, the value of k_y varied less than 2% for the different surface conditions tested and increased 9-11% when bonded to the surface.

A comparison of the lateral stiffness results with the fore-aft stiffness results indicates that, generally, the effects of testing techniques on these two mechanical properties are similar in nature, although the degree of influence on fore-aft properties appear to be greater. Thus, the observations and recommendations made for fore-aft stiffness can also be made for lateral stiffness.

Vertical Stiffness

The test apparatus used to obtain vertical stiffness data for the model tires is shown in Figure 17. This apparatus is yet another adaptation of the Static Testing Device described in [1]. In its use as a vertical stiffness test stand, the wheel and yoke were rigidly blocked up off the movable bearing plate. A "vertical" load was then applied horizontally to the tire by loading a rigid vertical surface against the tire. The vertical wall was attached to the bearing plate and the load was applied through the screw mechanism. The resulting "vertical" deflection was measured by the LVDT mounted between the bearing plate and the yoke. The force was measured with the same force

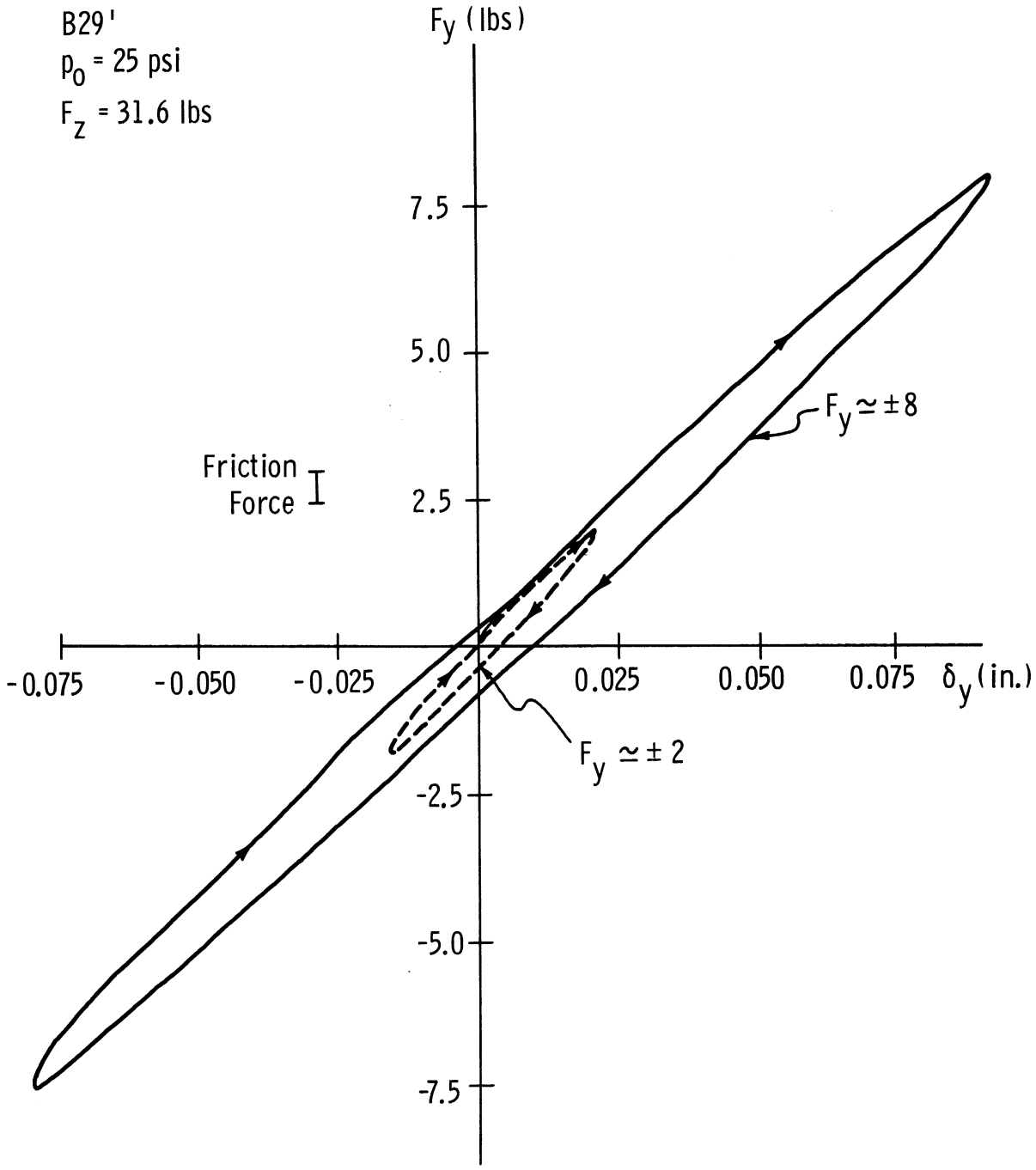

Figure 14. Lateral force-deflection loops illustrating effect of loop size for a model tire.

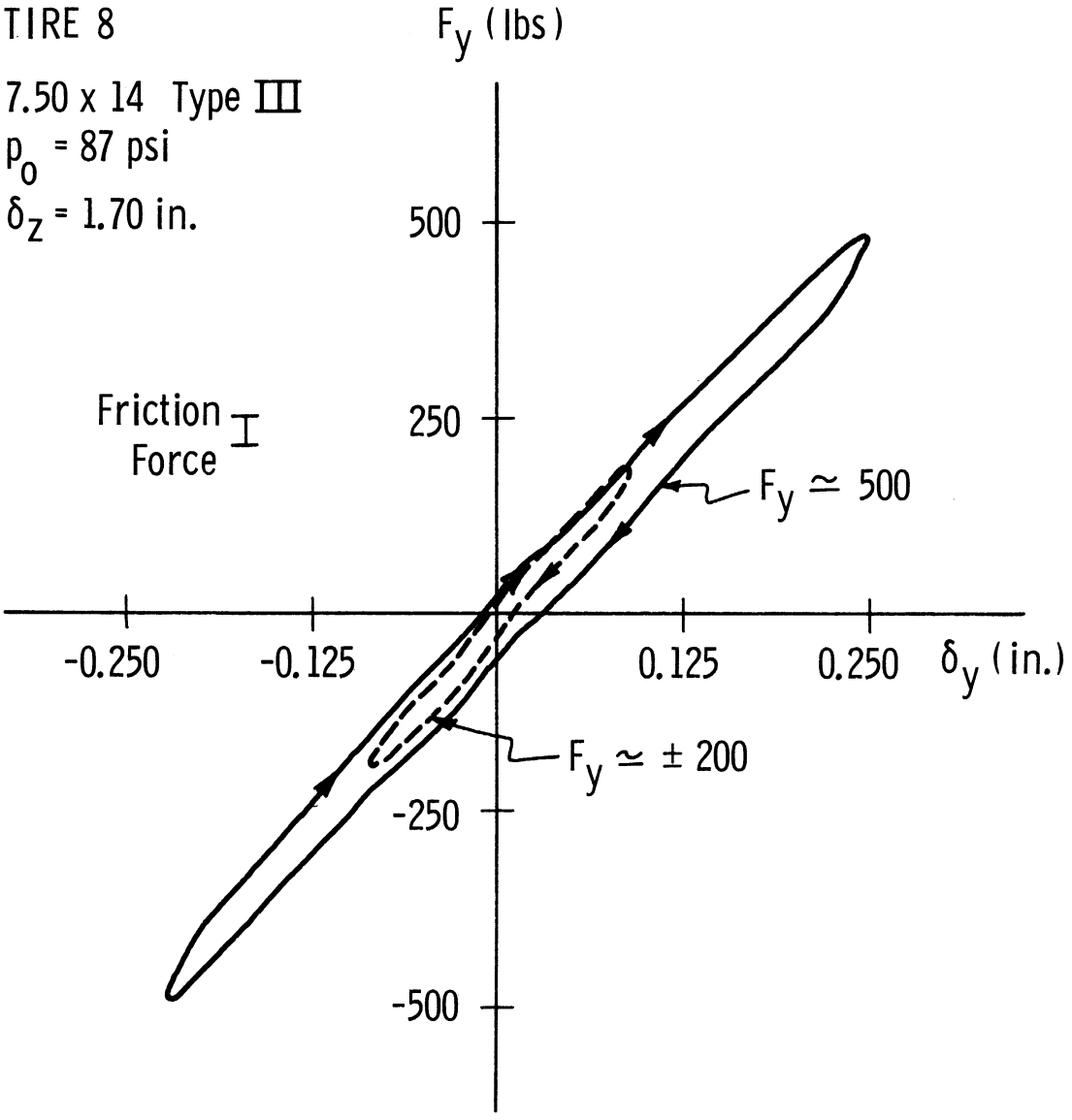

Figure 15. Lateral force-deflection loops illustrating effect of loop size for a full size tire.

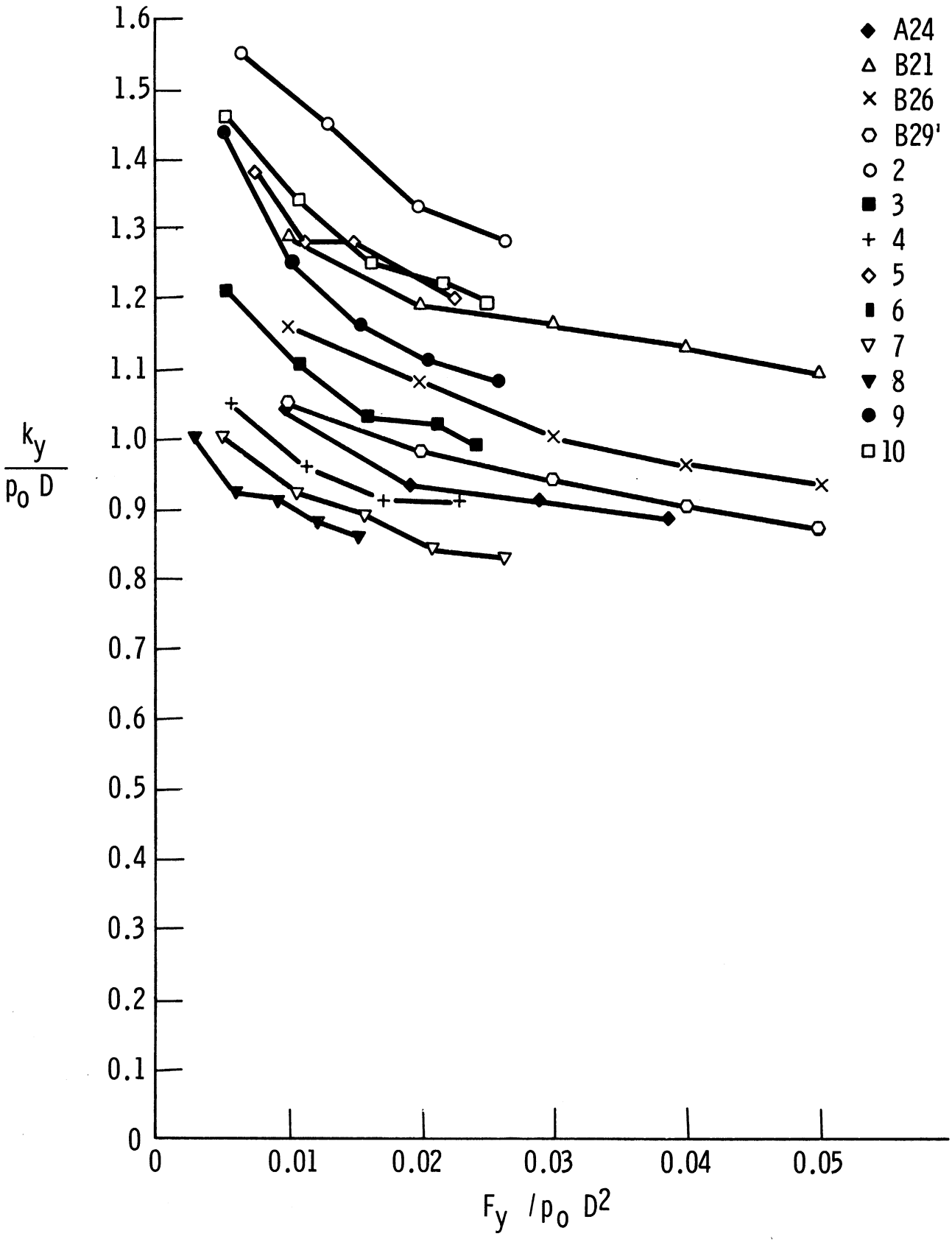

Figure 16. Dimensionless plot of lateral stiffness versus loop size for all tires.

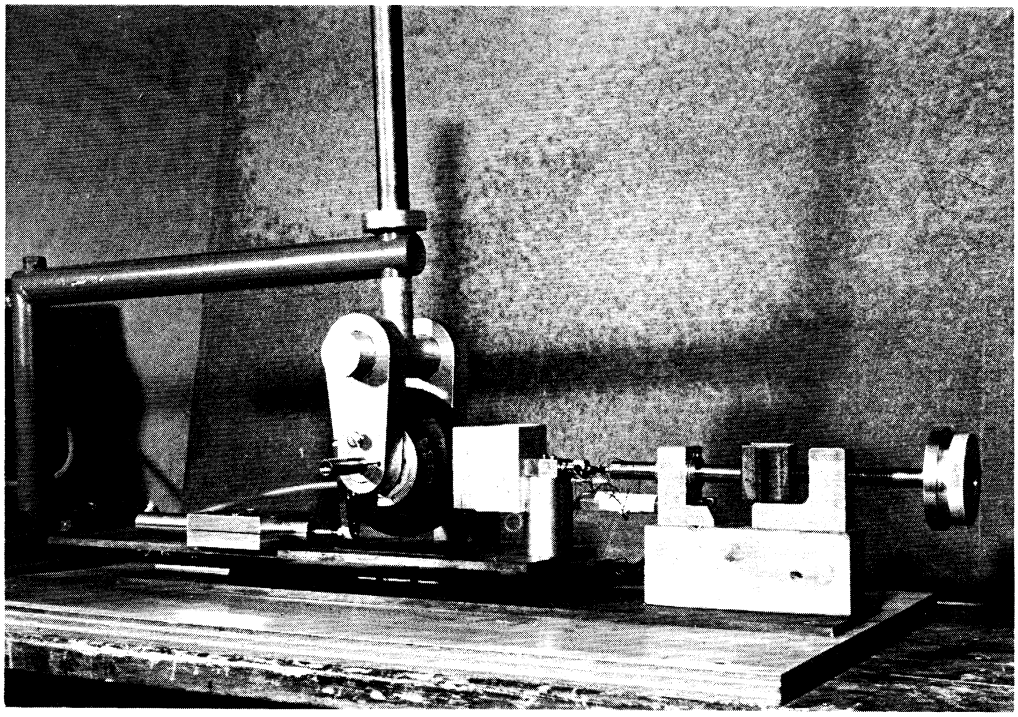

Figure 17. Photograph of vertical test apparatus for model tires.

transducer used for the previous tests. Again the output signals of the transducers were amplified and recorded on an x-y plotter.

The Riehle test machine used to obtain vertical stiffness for the full size tires was basically that illustrated in Figure 3. In this test the vertical load was applied through the movable loading head of the test machine and the resulting vertical deflection measured with a dial gage. For the vertical tests, four testing techniques were used to obtain vertical stiffness data. These techniques are described below as Tests A, B, C, and D.

Test A - Increment deflections.

The tire was inflated to the value listed in Table II. An increment of vertical deflection was applied and held constant for one minute at which time the vertical load was recorded. An identical increment of deflection was then applied and the procedure repeated. This test procedure was continued until

the maximum desired deflection was obtained. The increment deflections were then decreased to zero. The value of the vertical stiffness k_z was then determined by measuring the slope of the line joining the maximum end point of the force-deflection loop and the point whose coordinates were one half the maximum deflection and the average force of the increasing and decreasing portions of the loop at this deflection.

Test B - Continuous slow loop.

This test was a repeat of Test A except the vertical deflection was applied in a continuous manner. The time for one complete cycle was at least one minute.

Test C - Continuous fast loop.

This test was a repeat of Test B except the loop was complete in approximately 15 seconds.

Test D - Looping about a predeflection.

The tire was inflated to the specified value in Table II and deflected to one half of its maximum vertical deflection δ_{zm}. This deflection was taken as the center of a force-deflection loop. The loop was obtained by starting at this point as zero reference and slowly and continuously applying an increasing vertical deflection to a value short of δ_{zm} and then decreasing the deflection back through the reference point towards the real zero deflection, but reversing the deflection before zero was reached and increasing the deflection to the reference point. The value of k_z was then determined by measuring the slope of the line joining the end points of the loop.

A summary of the results from these four tests is shown in Table V. Again

TABLE V

SUMMARY OF STATIC VERTICAL STIFFNESS

k_z (lb/in.)

Tires	Test A		Test B		Test C		Test D	
	$\frac{F_{zm}}{\delta_{zm}}$	k_z	$\frac{F_{zm}}{\delta_{zm}}$	k_z	$\frac{F_{zm}}{\delta_{zm}}$	k_z	$\frac{F_{zm}}{\delta_{zm}}$	k_z
A24	140	160	140	160	140	160	150	160
B21	170	220	170	220	170	220	180	210
B26	180	230	180	230	180	230	190	220
B29'	180	230	190	240	190	240	200	230
1	2630	3260	2660	3260	2650	3240	2890	3290
2	1000	1210	1030	1290	1040	1300	1180	1320
3	1030	1200	1050	1260	1060	1260	1130	1290
4	810	900	810	900	820	920	850	920
5	750	840	760	870	780	900	850	880
6	610	690	610	700	620	720	660	700
7	840	950	850	980	860	970	920	990
8	3060	4070	3090	4120	3130	3980	3420	4140
9	1210	1470	1220	1500	1240	1570	1320	1580
10	1380	1410	1400	1460	1420	1460	1550	1490

some general observations can be made. First, in general, the variation of the values of k_z from Test A through Test D was less than 5%. Secondly, in general, the ratio of the maximum load to the maximum deflection, F_{zm}/δ_{zm}, was appreciably less (5-20%) than the value of k_z. See the results of Tests A, B, and C. This result is clearly indicated in Figures 18 and 19, which show typical vertical force-deflection curves for the model and full size tires, respectively. In these figures a definite nonlinearity is evident in the lower portion of the curve. This nonlinearity diminishes as the contact patch becomes fully developed under the influence of the vertical deflection. Thus, the ratio of F_{zm}/δ_{zm} was less than k_z because the F_z was proportionately smaller for the first half of the loop than for the second half.

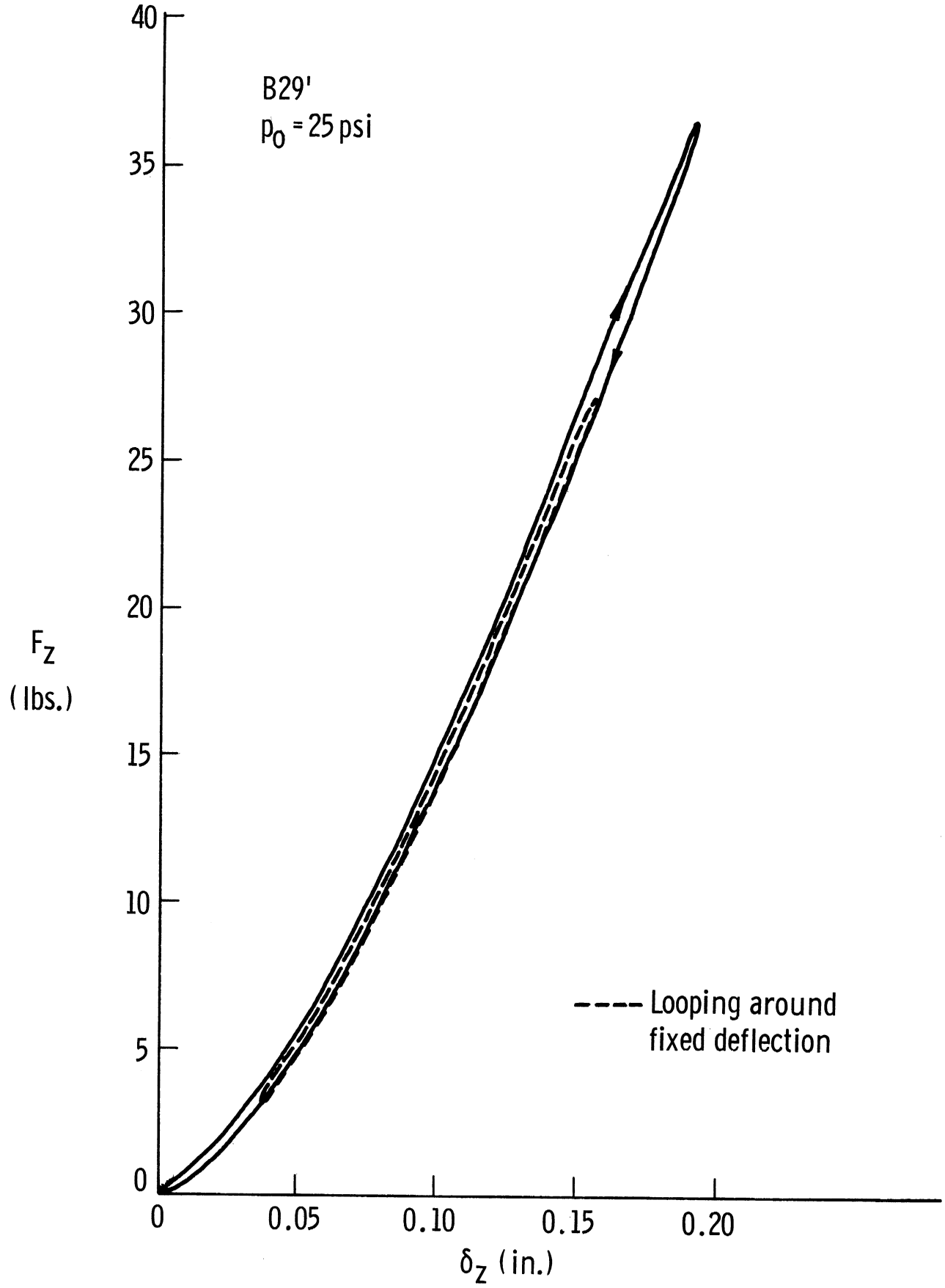

Figure 18. Typical vertical force-deflection loop for a model tire.

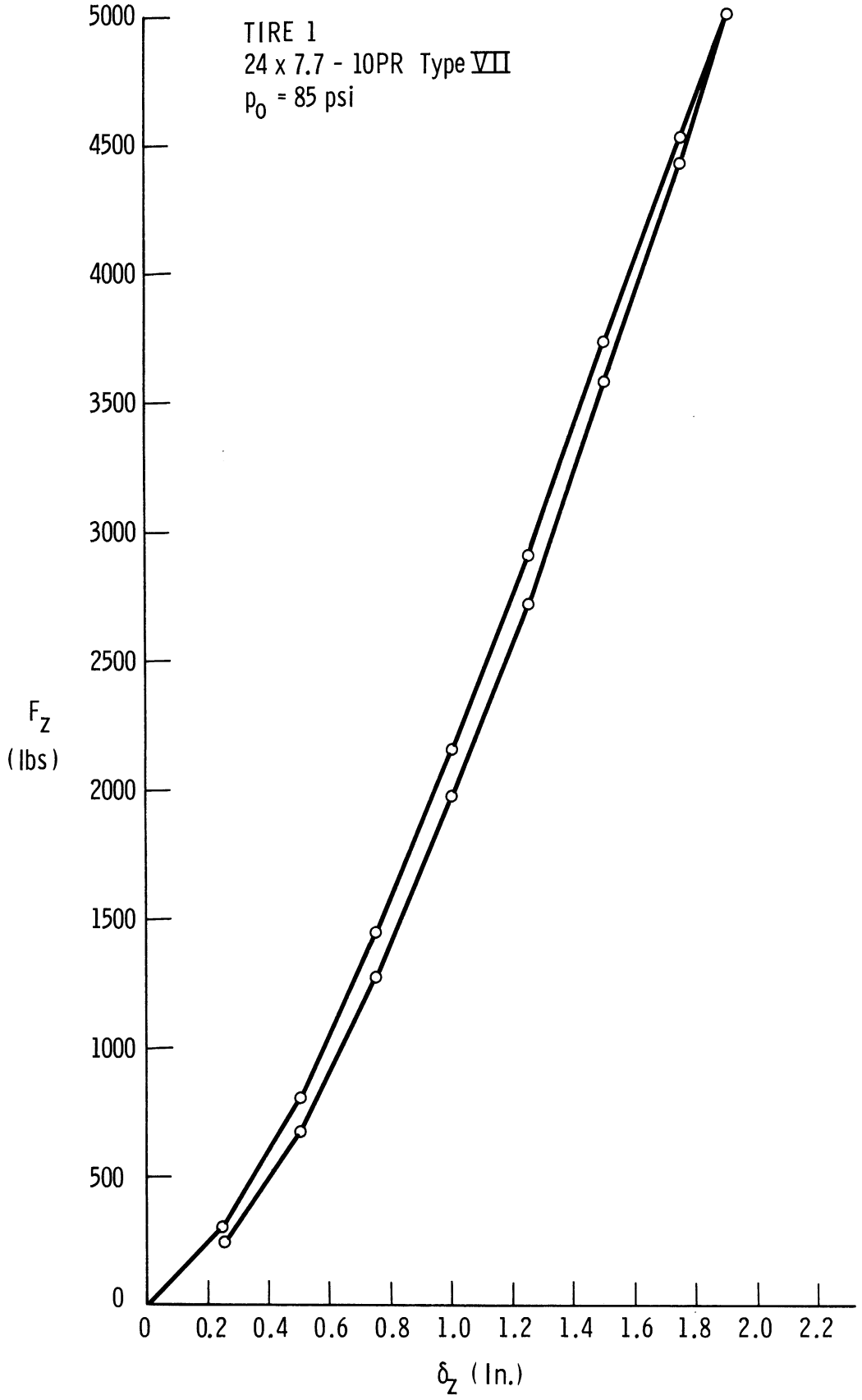

Figure 19. Typical vertical force-deflection loop for a full size tire.

Finally, the value of k_z was not appreciably changed when determined from the slope of the line through the end points of the loop generated by cycling about $\delta_{zm}/2$. This result is obvious after observing a typical loop and its corresponding full loop shown in Figure 18. It is evident in this figure that looping about a predeflection point does not effect the value of k_z as long as the loop does not extend significantly into the lower nonlinear region.

From these observations it might be recommended that the most consistent way to evaluate k_z is to establish a definition which will eliminate the initial "soft" portion of the vertical load-deflection curve, such as the definition of k_z used in this study. The technique used to obtain the force-deflection information seems to make little or no different in the value for k_z.

CONCLUDING REMARKS

The research program described in this paper indicates that testing techniques do have an effect on the measured values of the three static stiffnesses studied. As more tire user groups demand to know more tire characteristics, the need for a uniform criteria to measure and interpret values for these tire characteristics grows. It is hoped that this study might be used as a preliminary indication of how such a criteria may be formulated. Eventually, slow rolling properties such as cornering power, self-aligning torque, pneumatic trail, and relaxation length must also be exhaustively studied if the values of these tire parameters are to have meaning to the tire user group. However, the basic static tire properties covered in this report are probably the most amenable to some sort of measurement and interpretation standard. It is hoped that the results given in this report might provide some indication of the type of measurement and the difficulties of measurement interpretation that must be thoroughly investigated before such a standard can be proposed.

REFERENCE

[1] Clark, S. K., Dodge, R. N., Lackey, J. I., and Nybakken, G. H., "Structual Modeling of Aircraft Tires," NASA CR-2220, National Aeronautics and Space Administration, Washington, D. C., 1973.

DISTRIBUTION LIST

Agency	No. of Copies
Scientific and Technical Information Division Code US National Aeronautics and Space Administration Washington, D.C. 20546	25
NASA Headquarters Langley Research Center Dynamic Loads Division Hampton, Virginia 23365 Attn: Mr. Walter B. Horne	5